Prepared for submission to JHEP

Quark Number Susceptibilities from Two-Loop Hard Thermal Loop Perturbation Theory

Najmul Haque,[a] **Munshi G. Mustafa,**[a] **Michael Strickland**[b]

[a] *Theory Division, Saha Institute of Nuclear Physics, Kolkata, India - 700064*
[b] *Physics Department, Kent State University, Kent, OH 44242 United States*

Abstract: We use the recently obtained two-loop hard thermal loop perturbation theory thermodynamics functions of a plasma of quarks and gluons to compute the diagonal second- and fourth-order quark number susceptibilities. The two-loop hard thermal loop perturbation theory thermodynamic functions used are reliable in the limit that the ratio of the quark chemical potential to temperature is small. Using this result, we are able to obtain (semi-)analytic expressions for the quark number susceptibilities at leading- and next-to-leading-order in hard thermal loop perturbation theory. We compare the hard thermal loop perturbation theory results with perturbative quantum chromodynamics calculations, a Polyakov-loop Nambu-Jona-Lasinio calculation, and lattice quantum chromodynamics results. Finally, we introduce a prescription for avoiding over-counting in fixed-loop-order hard-thermal-loop perturbation theory results for the quark number susceptibilities.

Contents

1 Introduction **1**

2 Hard Thermal Loop Perturbation Theory **3**

3 Leading- and Next-to-leading-order HTLpt Pressure **3**
- 3.1 LO Pressure 3
- 3.2 NLO HTLpt Pressure and Variational Mass Gap Equations 4

4 Quark Number Susceptibility **7**
- 4.1 LO HTLpt second-order QNS 7
- 4.2 LO HTLpt fourth-order QNS 7
- 4.3 NLO HTLpt second-order QNS 8
- 4.4 Fourth-order QNS in NLO 8
- 4.5 Results and Discussions 9

5 Conclusion and Outlook **14**

1 Introduction

Dynamical chiral symmetry breaking and confinement are two well-known fundamental features of quantum chromodynamics (QCD). Nowadays it is generally believed that at high temperature and/or baryonic density strongly interacting matter will undergo chiral symmetry restoration and deconfinement phase transitions to a state of matter called the quark-gluon plasma (QGP). The study of such phase transitions has become a field of both theoretical and experimental interest since information about these phase transitions has the potential to provide a more fundamental understanding of QCD itself. In recent years, considerable effort has been dedicated to the creation of a QGP in the laboratory. The collider experiments currently dedicated to this search are the Relativistic Heavy Ion Collider (RHIC) at Brookhaven National Lab (BNL) and the Large Hadron Collider (LHC) at the European Organization for Nuclear Research (CERN). Future experiments are planned at the Facility for Antiproton and Ion Research (FAIR) at the Gesellschaft für Schwerionenforschung (GSI) facility. In all cases experimentalists collide heavy ions which have been accelerated to relativistic speeds in order to create the conditions necessary for the creation of a short-lived quark-gluon plasma.

In the confined/chiral-symmetry-broken phase, quarks are confined inside hadrons which possess integer-valued baryon number. In the deconfined/chiral-symmetry-restored phase, quarks which have fractional baryon number are free to propagate over larger distance scales. This fundamental difference leads to different quark number fluctuations in

the two phases [1]. In general, fluctuations of conserved quantities [2], such as baryon number, electric charge, strangeness, isospin charge, etc. are considered to be an important diagnostic tool for investigating the quark-hadron phase transition in relativistic heavy ion collisions [3, 4]. The magnitude of quark number fluctuations can be determined by computing the quark number susceptibilities (QNS), which measure the response of the quark number density to an infinitesimal change in the quark chemical potential in the limit of zero chemical potential. In addition, it was also argued recently that the QNS may be used to identify the position of the critical end point in the QCD phase diagram [5]. The QNS have been extensively studied in the last two decades using a variety of approaches including perturbative QCD (pQCD) [3, 6–8], lattice QCD (LQCD) simulations [9–17], Nambu-Jona-Lasinio (NJL) models [4, 18, 19], Polyakov Loop-Nambu-Jona-Lasinio (PNJL) models [19–22], hard-thermal/dense-loop (HTL/HDL) resummation techniques [23–27], rainbow-ladder and beyond-rainbow-ladder approximations of the Dyson-Schwinger equations [28], strong-coupling techniques [29], functional renormalisation group techniques [30], and quasiparticle models [31].

In view of the ongoing experimental and theoretical effort to understand the phase structure of QCD, the determination of QNS using a variety of approaches is important. Although the study of QCD matter very close to the phase transition requires a nonperturbative description, it is also interesting to explore the behavior of QNS beyond leading order (LO) [23–27] within weak coupling expansions which employ state-of-the-art resummation techniques [32–36]. Unlike LQCD, the weak-coupling expansion can straightforwardly handle finite density and temperature. As a result, such calculations can provide useful information about QNS. Herein we will assume massless quarks. For massless quark flavors the QNS are usually defined as

$$\chi_n(T) \equiv \left.\frac{\partial^n \mathcal{P}}{\partial \mu^n}\right|_{\mu=0} , \tag{1.1}$$

where $\mathcal{P}$ is the pressure of system, μ is the quark chemical potential and T is the temperature of the system. Above, n is the order of the QNS and we note that all odd orders vanish at $\mu = 0$ due to the charge-parity symmetry of the system. The equation of state (EOS) expressed in terms of the pressure $\mathcal{P}$ of QCD matter at high temperature and density is an important quantity, which we have recently computed to next-to-leading order (NLO) [37] at nonzero μ and T employing the hard thermal loop perturbation theory (HTLpt) reorganization of finite temperature QCD [32–36]. In this paper we compute the second- and fourth-order QNS from the LO and NLO HTLpt pressure and compare our results with conventional perturbative QCD calculations, various LQCD results, and a Polyakov-loop Nambu-Jona-Lasinio model.

The paper is organised as follows: In Sec. 2 we briefly review the HTLpt formalism. In Sec. 3 we present (semi-)analytic expressions for the LO and NLO HTLpt pressure. In Sec. 4 the second- and fourth-order QNS at LO and NLO are derived. The corresponding results are discussed and compared with first principles LQCD calculations, conventional pQCD, and a PNJL model. We conclude and give an outlook for future work in Sec. 5.

2 Hard Thermal Loop Perturbation Theory

HTL perturbation theory [34–36] is a reorganization of the perturbation series for hot and dense QCD which has the following Lagrangian density

$$\mathcal{L} = \left(\mathcal{L}_{\rm QCD} + \mathcal{L}_{\rm HTL}\right)\Big|_{g\to\sqrt{\delta}g} + \Delta\mathcal{L}_{\rm HTL}\,, \tag{2.1}$$

where $\Delta\mathcal{L}_{\rm HTL}$ collects all necessary additional HTL renormalization counterterms and $\mathcal{L}_{\rm HTL}$ is the HTL effective Lagrangian [32, 33]. The HTL effective Lagrangian can be written compactly as

$$\mathcal{L}_{\rm HTL} = -\frac{1}{2}(1-\delta)m_D^2 {\rm Tr}\left(G_{\mu\alpha}\left\langle\frac{y^\alpha y^\beta}{(y\cdot D)^2}\right\rangle_y G^\mu{}_\beta\right) + (1-\delta)\, i m_q^2 \bar{\psi}\gamma^\mu\left\langle\frac{y^\mu}{y\cdot D}\right\rangle_y \psi\,, \tag{2.2}$$

where D is the covariant derivative, $y=(1,\mathbf{y})$ is a light like vector and $\langle\cdots\rangle$ is the average over all possible directions, $\hat{y}$, of the loop momenta. The HTL effective action is gauge invariant, nonlocal, and can generate all HTL n-point functions [32, 33], which satisfy the necessary Ward-Takahashi identities by construction. The mass parameters m_D and m_q are the Debye gluon screening and quark masses in a hot and dense medium, respectively, which depend on the strong coupling g, the temperature T, and the chemical potential μ. In the end we will formally treat the masses m_D and m_q in (2.2) as being leading-order in g in order to make the calculation tractable [34–36]. The $n^{\rm th}$ loop order in the HTLpt loop expansion is obtained by expanding the partition function through order δ^{n-1} and then taking $\delta\to 1$ [23, 24, 26, 27, 34–38]. In higher order calculations, one usually fixes the parameters m_D and m_q by employing a variational prescription which requires that the first derivative of the pressure with respect to both m_D and m_q vanishes such that the free energy is minimized [34, 35, 37]. In the following section, we briefly describe the recently computed finite temperature and chemical potential NLO HTLpt pressure [37].

3 Leading- and Next-to-leading-order HTLpt Pressure

Using the above reorganization of finite temperature/density QCD, the two-loop pressure for a plasma of quarks and gluons can be obtained in HTLpt by expanding in the ratio of chemical potential to temperature through fourth order in μ/T. Below we quote both leading-order (LO) and next-to-leading-order (NLO) expressions for the pressure, along with the relevant mass gap equations, which are then used to compute NLO QNS at various orders. The calculation of the LO and NLO HTLpt pressure at finite temperature and chemical potential was presented in an earlier paper [37] and we refer the reader to this paper for the detailed calculation.

3.1 LO Pressure

The LO HTLpt pressure through $\mathcal{O}(g^4)$ at any μ is [27, 37]

$$\begin{aligned}\mathcal{P}_{\rm LO} = d_A\frac{\pi^2T^4}{45}\Bigg\{1 + \frac{7}{4}\frac{d_F}{d_A}\left(1+\frac{120}{7}\hat{\mu}^2+\frac{240}{7}\hat{\mu}^4\right) - \frac{15}{2}\hat{m}_D^2 - 30\frac{d_F}{d_A}\left(1+12\hat{\mu}^2\right)\hat{m}_q^2 \\ + 30\hat{m}_D^3 + \frac{45}{4}\left(\ln\frac{\hat{\Lambda}}{2} - \frac{7}{2} + \gamma + \frac{\pi^2}{3}\right)\hat{m}_D^4 - 60\frac{d_F}{d_A}(\pi^2-6)\hat{m}_q^4\Bigg\}\,.\end{aligned} \tag{3.1}$$

Note that apart from the free contribution, no explicit terms proportional to $\hat{\mu}^4$ appear through $\mathcal{O}(\hat{m}_q^4)$. The dimensionless variables $\hat{m}_D$, $\hat{m}_q$, $\hat{\Lambda}$, and $\hat{\mu}$ are defined as

$$\hat{m}_D = \frac{m_D}{2\pi T}\,, \quad \hat{m}_q = \frac{m_q}{2\pi T}\,, \quad \hat{\Lambda} = \frac{\Lambda}{2\pi T}\,, \quad \hat{\mu} = \frac{\mu}{2\pi T}\,. \tag{3.2}$$

At leading order, the weak coupling expressions for the mass parameters are

$$m_D^2 = \frac{g^2T^2}{3}\left[c_A + s_F\left(1+12\hat{\mu}^2\right)\right]\,; \quad m_q^2 = \frac{g^2T^2}{4}\frac{c_F}{2}\left(1+4\hat{\mu}^2\right)\,. \tag{3.3}$$

In the expressions for the pressure and masses above we use the standard notation for the various Casimir invariants necessary: $d_F = N_c N_f$, $d_A = N_c^2 - 1$, $s_F = N_f/2$, $c_A = N_c$ and $c_F = (N_c^2-1)/2N_c$. At LO the variational method for fixing the mass parameters m_D and m_q can not be used in practice, since it results in only the trivial solution $m_D = m_q = 0$. Instead at LO one canonically uses the LO masses listed in Eqs. (3.3) as the lowest order "variational solutions" for the mass parameters.

3.2 NLO HTLpt Pressure and Variational Mass Gap Equations

The NLO HTLpt pressure through $\mathcal{O}[(\mu/T)^4]$ is [37]

$$\begin{aligned}
\mathcal{P}_{\rm NLO} = d_A\frac{\pi^2T^4}{45}\Bigg\{&1+\frac{7}{4}\frac{d_F}{d_A}\left(1+\frac{120}{7}\hat{\mu}^2+\frac{240}{7}\hat{\mu}^4\right)-15\hat{m}_D^3\\
&-\frac{45}{4}\left(\log\frac{\hat{\Lambda}}{2}-\frac{7}{2}+\gamma+\frac{\pi^2}{3}\right)\hat{m}_D^4+60\frac{d_F}{d_A}\left(\pi^2-6\right)\hat{m}_q^4\\
&+\frac{\alpha_s}{\pi}\Bigg[-\frac{5}{4}\left(c_A+\frac{5}{2}s_F\left(1+\frac{72}{5}\,\hat{\mu}^2+\frac{144}{5}\,\hat{\mu}^4\right)\right)+15\left(c_A+s_F(1+12\hat{\mu}^2)\right)\hat{m}_D\\
&\quad-\frac{55}{4}\Bigg\{c_A\left(\log\frac{\hat{\Lambda}}{2}-\frac{36}{11}\log\hat{m}_D-2.001\right)-\frac{4}{11}s_F\Bigg[\left(\log\frac{\hat{\Lambda}}{2}-2.333\right)\\
&\qquad+\left(24-18\zeta(3)\right)\left(\log\frac{\hat{\Lambda}}{2}-15.662\right)\hat{\mu}^2\\
&\qquad\quad+120\left(\zeta(5)-\zeta(3)\right)\left(\log\frac{\hat{\Lambda}}{2}-1.0811\right)\hat{\mu}^4+\mathcal{O}\left(\hat{\mu}^6\right)\Bigg]\Bigg\}\hat{m}_D^2\\
&-45\,s_F\left\{\log\frac{\hat{\Lambda}}{2}+2.198-44.953\hat{\mu}^2-\left(288\ln\frac{\hat{\Lambda}}{2}+19.836\right)\hat{\mu}^4+\mathcal{O}\left(\hat{\mu}^6\right)\right\}\hat{m}_q^2\\
&+\frac{165}{2}\Bigg\{c_A\left(\log\frac{\hat{\Lambda}}{2}+\frac{5}{22}+\gamma\right)\\
&-\frac{4}{11}s_F\left(\log\frac{\hat{\Lambda}}{2}-\frac{1}{2}+\gamma+2\ln 2-7\zeta(3)\hat{\mu}^2+31\zeta(5)\hat{\mu}^4+\mathcal{O}\left(\hat{\mu}^6\right)\right)\Bigg\}\hat{m}_D^3\\
&+30s_F\left(\frac{\zeta'(-1)}{\zeta(-1)}+\ln\hat{m}_D\right)\left[(24-18\zeta(3))\hat{\mu}^2+120(\zeta(5)-\zeta(3))\hat{\mu}^4+\mathcal{O}\left(\hat{\mu}^6\right)\right]\hat{m}_D^3\\
&+180\,s_F\hat{m}_D\hat{m}_q^2\Bigg]\Bigg\}\,,
\end{aligned} \tag{3.4}$$

which is accurate up to $\mathcal{O}(g^3)$ and nominally accurate to $\mathcal{O}(g^5)$ since it was obtained from an expansion of two-loop thermodynamic potential in a power series in m_D/T and m_q/T treating both m_D and m_q having leading terms proportional to g. Using the result above, the mass parameters m_D and m_q can be obtained using the variational prescription

$$\left.\frac{\partial}{\partial m_D}\mathcal{P}_{\rm NLO}\right|_{m_q=const.} = 0 \qquad \text{and} \qquad \left.\frac{\partial}{\partial m_q}\mathcal{P}_{\rm NLO}\right|_{m_D=const.} = 0\,, \tag{3.5}$$

which leads to two gap equations for m_D and m_q, respectively

$$\begin{aligned}
&45\hat{m}_D^2\left[1+\left(\ln\frac{\hat{\Lambda}}{2}-\frac{7}{2}+\gamma+\frac{\pi^2}{3}\right)\hat{m}_D\right]\\
&=\frac{\alpha_s}{\pi}\Bigg\{15(c_A+s_F(1+12\hat{\mu}^2))-\frac{55}{2}\left[c_A\left(\ln\frac{\hat{\Lambda}}{2}-\frac{36}{11}\ln\hat{m}_D-3.637\right)\right.\\
&-\frac{4}{11}s_F\left\{\ln\frac{\hat{\Lambda}}{2}-2.333+(24-18\zeta(3))\left(\ln\frac{\hat{\Lambda}}{2}-15.662\right)\hat{\mu}^2\right.\\
&+\left.\left.120(\zeta(5)-\zeta(3))\left(\ln\frac{\hat{\Lambda}}{2}-1.0811\right)\hat{\mu}^4\right\}\right]\hat{m}_D+\frac{495}{2}\left[c_A\left(\ln\frac{\hat{\Lambda}}{2}+\frac{5}{22}+\gamma\right)\right.\\
&-\frac{4}{11}s_F\left\{\ln\frac{\hat{\Lambda}}{2}-\frac{1}{2}+\gamma+2\ln 2-7\zeta(3)\hat{\mu}^2+31\zeta(5)\hat{\mu}^4\right.\\
&-\left.\left.\left(\frac{\zeta'(-1)}{\zeta(-1)}+\ln m_D+\frac{1}{3}\right)\left((24-18\zeta(3))\hat{\mu}^2+120(\zeta(5)-\zeta(3))\hat{\mu}^4\right)\right\}\right]m_D^2+180s_F\hat{m}_q^2\Bigg\},
\end{aligned} \tag{3.6}$$

and

$$\begin{aligned}
\hat{m}_q^2=\frac{d_A}{8d_F\,(\pi^2-6)}\frac{\alpha_s s_F}{\pi}\Bigg[3\Bigg(&\ln\frac{\hat{\Lambda}}{2}+2.198-44.953\;\hat{\mu}^2\\
&-\left(288\ln\frac{\hat{\Lambda}}{2}+19.836\right)\hat{\mu}^4\Bigg)-12\hat{m}_D\Bigg].
\end{aligned} \tag{3.7}$$

To obtain the second and fourth-order quark number susceptibilities in HTLpt, one requires expressions for m_D, $\frac{\partial^2}{\partial\mu^2}m_D$, m_q, and $\frac{\partial^2}{\partial\mu^2}m_q$ at $\mu=0$ from Eqs. (3.6) and (3.7).[1] We list these here for completeness. The result for the limit of the m_D gap equation

[1]Note that odd derivatives with respect to μ vanish at $\mu=0$. Fourth-order derivatives at $\mu=0$ are nonzero, however, they appear as multiplicative factors of the gap equations and are therefore not required, as we will see below.

necessary is

$$
\begin{aligned}
&45\hat{m}_D^2(0)\left[1+\left(\ln\frac{\hat{\Lambda}}{2}-\frac{7}{2}+\gamma+\frac{\pi^2}{3}\right)\hat{m}_D(0)\right]\\
&=\frac{\alpha_s}{\pi}\Bigg\{15(c_A+s_F)-\frac{55}{2}\left[c_A\left(\ln\frac{\hat{\Lambda}}{2}-\frac{36}{11}\ln\hat{m}_D(0)-3.637\right)\right.\\
&-\left.\frac{4}{11}s_F\left\{\ln\frac{\hat{\Lambda}}{2}-2.333\right\}\right]\hat{m}_D(0)+\frac{495}{2}\left[c_A\left(\ln\frac{\hat{\Lambda}}{2}+\frac{5}{22}+\gamma\right)\right.\\
&-\left.\frac{4}{11}s_F\left(\ln\frac{\hat{\Lambda}}{2}-\frac{1}{2}+\gamma+2\ln 2\right)\right]m_D^2(0)+180s_F\hat{m}_q^2(0)\Bigg\}.
\end{aligned}
\tag{3.8}
$$

For m_q one obtains

$$
\hat{m}_q^2(0)=\frac{d_A}{8d_F\left(\pi^2-6\right)}\frac{\alpha_s s_F}{\pi}\left[3\left(\ln\frac{\hat{\Lambda}}{2}+2.198\right)-12\hat{m}_D(0)\right]. \tag{3.9}
$$

For $\frac{\partial^2}{\partial\mu^2}m_D$ one obtains

$$
\begin{aligned}
&45\left[2+3\left(\ln\frac{\hat{\Lambda}}{2}-\frac{7}{2}+\gamma+\frac{\pi^2}{3}\right)m_D(0)\right]m_D(0)m_D''(0)\\
&=\frac{\alpha_s}{\pi}\Bigg\{360s_F-\frac{55}{2}m_D''(0)\left[c_A\left(\ln\frac{\hat{\Lambda}}{2}-\frac{36}{11}\ln\hat{m}_D(0)-6.9097\right)-\frac{4}{11}s_F\left(\ln\frac{\hat{\Lambda}}{2}-2.333\right)\right]\\
&+495m_D''(0)\left[c_A\left(\frac{5}{22}+\gamma+\ln\frac{\hat{\Lambda}}{2}\right)-\frac{4}{11}s_F\left(\ln\frac{\hat{\Lambda}}{2}-\frac{1}{2}+\gamma+2\ln 2\right)\right]\hat{m}_D(0)\\
&+20s_F\left(\ln\frac{\hat{\Lambda}}{2}-15.662\right)(24-18\zeta(3))\hat{m}_D(0)\\
&+180s_F\hat{m}_D(0)^2\left[7\zeta(3)+\left(\frac{\zeta'(-1)}{\zeta(-1)}+\ln\hat{m}_D(0)+\frac{1}{3}\right)(24-18\zeta(3))\right]\\
&+360s_F\hat{m}_q(0)\hat{m}_q''(0)\Bigg\}.
\end{aligned}
\tag{3.10}
$$

For $\frac{\partial^2}{\partial\mu^2}m_q$ one obtains

$$
\hat{m}_q(0)\hat{m}_q''(0)=-\frac{3d_A}{8d_F\left(\pi^2-6\right)}\frac{\alpha_s s_F}{\pi}\left[44.953+2\hat{m}_D''(0)\right]. \tag{3.11}
$$

In the expressions above, $m_D(0)\equiv m_D(T,\Lambda,\mu=0)$, $m_D''(0)\equiv\frac{\partial^2}{\partial\mu^2}m_D(T,\Lambda,\mu)\Big|_{\mu=0}$ and similarly for m_q.

4 Quark Number Susceptibility

We are now in a position to obtain the second and fourth-order HTLpt QNS following Eq. (1.1). We also note that the pure gluonic loops at any order do not contribute to QNS, however, gluons contribute through the dynamical fermions through fermionic loops. This makes QNS proportional to only quark degrees of freedom. Below we present (semi-)analytic expressions for both LO and NLO QNS.

4.1 LO HTLpt second-order QNS

An analytic expression for the LO HTLpt second-order QNS can be obtained using Eq. (3.1)

$$\begin{aligned}\chi_2^{\rm LO}(T) &= \frac{\partial^2}{\partial\mu^2}\mathcal{P}_{\rm LO}(T,\Lambda,\mu)\bigg|_{\mu=0} = \frac{1}{(2\pi T)^2}\,\frac{\partial^2}{\partial\hat{\mu}^2}\mathcal{P}_{\rm LO}(T,\Lambda,\hat{\mu})\bigg|_{\hat{\mu}=0}\\ &= \frac{d_F T^2}{3}\Bigg[1-\frac{3c_F}{4}\left(\frac{g}{\pi}\right)^2+\frac{c_F}{4}\sqrt{3(c_A+s_F)}\left(\frac{g}{\pi}\right)^3-\frac{c_F^2}{64}\left(\pi^2-6\right)\left(\frac{g}{\pi}\right)^4\\ &\quad+\frac{c_F}{16}(c_A+s_F)\left(\log\frac{\hat{\Lambda}}{2}-\frac{7}{2}+\gamma+\frac{\pi^2}{3}\right)\left(\frac{g}{\pi}\right)^4\Bigg]\,,\end{aligned} \tag{4.1}$$

where the LO Debye and quark masses listed in Eqs. (3.3) and their μ derivatives have been used.

4.2 LO HTLpt fourth-order QNS

An analytic expression for the LO HTLpt fourth-order QNS can also be obtained using Eq. (3.1)

$$\begin{aligned}\chi_4^{\rm LO}(T) &= \frac{\partial^4}{\partial\mu^4}\mathcal{P}_{\rm LO}(T,\Lambda,\mu)\bigg|_{\mu=0} = \frac{1}{(2\pi T)^4}\,\frac{\partial^4}{\partial\hat{\mu}^4}\mathcal{P}_{\rm LO}(T,\Lambda,\hat{\mu})\bigg|_{\hat{\mu}=0}\\ &= \frac{2d_F}{\pi^2}\Bigg[1-\frac{3}{4}c_F\left(\frac{g}{\pi}\right)^2+\frac{3}{8}c_F s_F\sqrt{\frac{3}{c_A+s_F}}\left(\frac{g}{\pi}\right)^3-\frac{c_F^2\left(\pi^2-6\right)}{64}\left(\frac{g}{\pi}\right)^4\\ &\quad+\frac{3}{16}c_F s_F\left(\log\frac{\hat{\Lambda}}{2}-\frac{7}{2}+\gamma+\frac{\pi^2}{3}\right)\left(\frac{g}{\pi}\right)^4\Bigg]\,,\end{aligned} \tag{4.2}$$

where, once again, the LO Debye and quark masses listed in Eqs. (3.3) and their μ derivatives have been used. We note that both $\chi_2^{\rm LO}$ in (4.1) and $\chi_4^{\rm LO}$ in (4.2) are the same as those recently obtained by Andersen et al. [27]; however, the closed-form expressions obtained here have not been explicitly listed therein.

4.3 NLO HTLpt second-order QNS

A semi-analytic expression for the NLO HTLpt second-order QNS can be obtained from Eq. (3.4)

$$\begin{aligned}\chi_2^{\rm NLO}(T) &= \frac{\partial^2}{\partial\mu^2}\mathcal{P}_{\rm NLO}(T,\Lambda,\mu)\Big|_{\mu=0} = \frac{1}{(2\pi T)^2}\,\frac{\partial^2}{\partial\hat{\mu}^2}\mathcal{P}_{\rm NLO}(T,\Lambda,\hat{\mu})\Big|_{\hat{\mu}=0}\\ &= \frac{d_A T^2}{2}\left[\frac{2}{3}\frac{d_F}{d_A}+\frac{\alpha_s}{\pi}s_F\left\{-1+4\,\hat{m}_D(0)+\frac{2}{3}\left(\ln\frac{\hat{\Lambda}}{2}-15.662\right)(4-3\zeta(3))\,\hat{m}_D^2(0)\right.\right.\\ &\quad\left.\left.+\,44.953\,\hat{m}_q^2(0)+\left[\frac{14}{3}\zeta(3)+\left(\frac{\zeta'(-1)}{\zeta(-1)}+\ln\hat{m}_D(0)\right)(16-12\zeta(3))\right]\hat{m}_D^3(0)\right\}\right].\end{aligned} \tag{4.3}$$

We note that no μ derivatives of the mass parameters appear in (4.3) and, as a result, $\chi_2^{\rm NLO}(T)$ reduces to such a simple and compact form. This is because the second derivatives of the mass parameters with respect to μ always appear as multiplicative factors of the gap equations (3.8) and (3.9) and hence these contributions vanish. Numerically solving for the variational masses using Eq. (3.8) and (3.9) one can directly compute $\chi_2^{\rm NLO}(T)$ from (4.3). Alternatively, we have also computed $\chi_2^{\rm NLO}(T)$ by performing numerical differentiation of the pressure in (3.4) which leads to the same result within numerical errors.

4.4 Fourth-order QNS in NLO

A semi-analytic expression for the NLO HTLpt fourth-order QNS can also be obtained from Eq. (3.4)

$$\begin{aligned}\chi_4^{\rm NLO}(T) &= \frac{\partial^4}{\partial\mu^4}\mathcal{P}_{\rm NLO}(T,\Lambda,\mu)\Big|_{\mu=0} = \frac{1}{(2\pi T)^4}\,\frac{\partial^4}{\partial\hat{\mu}^4}\mathcal{P}_{\rm NLO}(T,\Lambda,\hat{\mu})\Big|_{\hat{\mu}=0}\\ &= \frac{d_A}{4\pi^2}\left[8\frac{d_F}{d_A}+8\frac{d_F}{d_A}(\pi^2-6)\hat{m}_q^2(0)\hat{m}_q''(0)^2+\frac{\alpha_s}{\pi}s_F\left\{-12+6\hat{m}_D''(0)\right.\right.\\ &\quad+3\hat{m}_D^2(0)\left[\left(\frac{\zeta'(-1)}{\zeta(-1)}+\ln\hat{m}_D(0)-\frac{1}{3}\right)(24-18\zeta(3))+7\zeta(3)\right]\hat{m}_D''(0)\\ &\quad+\hat{m}_D(0)\hat{m}_D''(0)\left(\ln\frac{\hat{\Lambda}}{2}-15.662\right)(8-6\zeta(3))+2(24-18\zeta(3))\hat{m}_D^2(0)\hat{m}_D''(0)\\ &\quad-4\hat{m}_D^3(0)\left[31\zeta(5)-120\left(\frac{\zeta'(-1)}{\zeta(-1)}+\ln\hat{m}_D(0)\right)(\zeta(5)-\zeta(3))\right]\\ &\quad+80\hat{m}_D^2(0)\left(\ln\frac{\hat{\Lambda}}{2}-1.0811\right)(\zeta(5)-\zeta(3))\\ &\quad+6\left[\left(19.836\;+288\ln\frac{\hat{\Lambda}}{2}\right)\hat{m}_q^2(0)+44.953\hat{m}_q(0)\hat{m}_q''(0)\right]\\ &\quad\left.\left.+6\hat{m}_D''(0)\hat{m}_q(0)\hat{m}_q''(0)\right\}\right],\end{aligned} \tag{4.4}$$

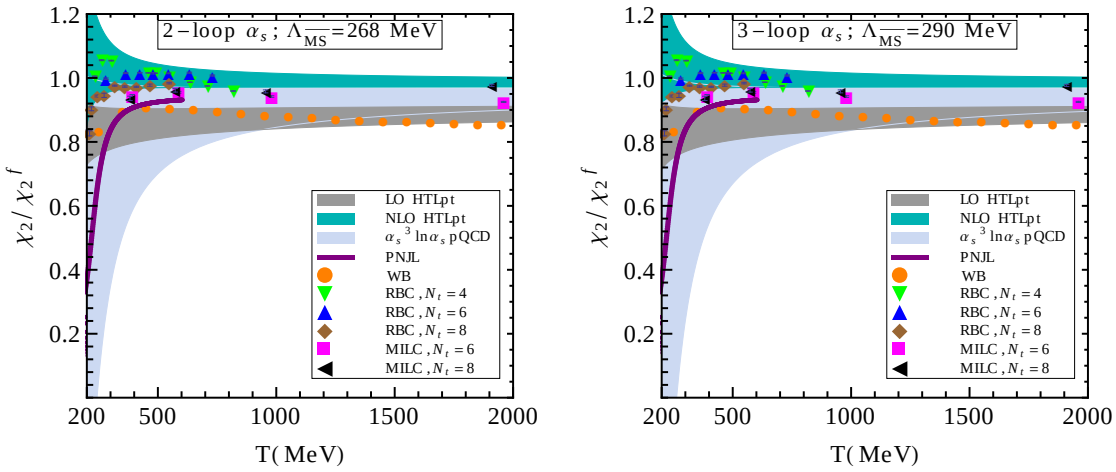

Figure 1. Left panel: χ_2 scaled by the free field value for LO (grey band) and NLO (sea green band) in 2-loop HTLpt, 4-loop pQCD (sky blue band) [8], LQCD (various symbols) [9, 11, 15], and PNJL model (thick purple line) [22] are plotted as a function of the temperature. The bands in HTLpt and pQCD are obtained by varying the $\overline{\rm MS}$ renormalisation scale (Λ) around its central value by a factor of two. We also used $\Lambda_{\overline{\rm MS}} = 268$ MeV and 2-loop α_s for HTLpt and pQCD. In the PNJL model [22] χ_2 is obtained using an eight-fermion interaction. The Wuppertal-Budapest (WB) group [9] data are obtained using the tree-level improved Symanzik action and a stout smeared staggered fermionic action with light quark masses $\sim 0.035\,m_s$, with m_s being the strange quark mass near its physical value. The RBC-Bielefeld collaboration [10] used a p4 action whereas the MILC collaboration [15] used an asqtad action. In both cases the light quark mass ranges from (0.1-0.2) m_s. Right panel: Same as left panel but using 3-loop α_s and $\Lambda_{\overline{\rm MS}} = 290$ MeV.

where the double derivatives of the mass parameters with respect to μ survive, but the fourth derivatives of the mass parameters disappear as discussed earlier. One can now directly compute the fourth-order susceptibility by using numerical solutions of the gap equations in (3.8) and (3.11). Alternatively, we have also computed $\chi_4^{\rm NLO}(T)$ by performing numerical differentiation of the pressure in (3.4) which leads to the same result within numerical errors.

4.5 Results and Discussions

Computing the different susceptibilities in HTLpt requires a choice of the renormalization scale Λ, the $\overline{\rm MS}$ momentum scale $\Lambda_{\overline{\rm MS}}$, and a specification of the order of the running coupling α_s used. In what follows we vary the renormalization scale Λ by a factor of two around a central value of $\Lambda = 2\pi T$ which results in a band that can be used to ascertain the level of minimal theoretical uncertainty. The value of $\Lambda_{\overline{\rm MS}}$ depends on the order of the running coupling chosen and we fix its value from a recent lattice QCD determination [39]. The specific value of $\Lambda_{\overline{\rm MS}}$ used in each case is specified in the figure captions.

In Fig. 1 we have plotted the $N_f = 3$ second-order QNS scaled by the corresponding free gas limit as a function of the temperature. As discussed above, the bands shown for the HTLpt and pQCD [8] results indicate the sensitivity of χ_2 to the choice of the renormali-

sation scale Λ. However, χ_2 in both HTLpt and pQCD depends only weakly on the chosen order of the running of the strong coupling and in turn only depends weakly on $\Lambda_{\overline{\rm MS}}$, as can be seen clearly from both panels of Fig. 1. The LO HTLpt prediction for χ_2 seems to agree reasonably well with the available Wuppertal-Budapest LQCD data;[2] however, there is a sizable variation among different lattice computations [9, 11, 15] considering improved lattice actions and a range of quark masses (see caption). However, lowering the quark mass ($\sim 0.035 m_s$, m_s is the strange quark mass) nearer to its physical value [9] seems to have a very small effect in the temperature range, as seen from the LQCD data. Note that for the Wuppertal-Budapest (WB) lattice data shown in Figs. 1 and 2, Ref. [9] provided a parameterization of their χ_2 data

$$\chi_2(T) = e^{-(h_3/t+h_4/t^2)}\, f_3\,[\tanh(f_4\, t + f_5) + 1]\,, \tag{4.5}$$

where $t = T/(200\ \text{MeV})$, $h_3 = -0.5022$, $h_4 = 0.5950$, $f_3 = 0.1359$, $f_4 = 6.3290$, and $f_5 = -4.8303$. The authors of Ref. [9] performed the fit for data in the temperature range $125\ \text{MeV} < T \leq 400\ \text{MeV}$. Using the parameterization above, we have extended their data up to 2000 MeV with a step size of 100 MeV in order to allow comparison with the HTLpt results at high temperature. The results for χ_2 obtained using a nonperturbative PNJL model [22] which includes an eight-quark interaction are only available very close to the phase transition temperature.

As discussed earlier, purely gluonic loops do not directly contribute to QNS, and instead contribute indirectly through dynamical quarks via internal quark loops which contribute to the gluonic Debye mass. The LO HTLpt result requires only a resummed HTL quark propagator, which in practice corresponds to static external quarks (valence quarks)[3] and thus there is no direct dynamical quark contribution in the LO QNS in (4.1) except what comes through the LO mass parameter m_D and its derivative in (4.1). We note here that $\chi_2^{\rm LO}$ in (4.1) overcounts the perturbative order g^2 due to the inclusion of the μ derivatives of the LO mass parameters m_q and m_D which violates the LO mass prescriptions as the lowest order variational solutions within one-loop HTLpt. The reason is the following: the mass term m_i^2/T^2 ($i = q,\, D$) in the one-loop pressure (3.1) contributes to LO QNS through the double derivative with respect to μ as $\sim [(m_i')^2 + m_i m_i''] = m_i m_i''$ as $m_i' \to 0$ as $\mu \to 0$. Now, $m_i m_i''$ is nonzero and finite at $\mu \to 0$, which is the source of over-counting. As an example, in LO m_D the μ dependence appears from a dynamical quark loop (internal quark loop in gluon propagator). The second derivative of such dynamical quarks at one-loop order leads to (i) a two-loop quark diagram with an internal gluon line, and (ii) a mixed two-loop diagram consisting of a pure quark and a pure gluon loop. Also, the double derivative of m_q with respect to μ corresponds to a two-loop quark diagram with two internal gluon lines. This would basically lead to higher order corrections to LO mass parameters m_D and m_q which would then spoil the LO order mass approximation as the lowest order variational solution. Therefore, taking into account the contribution of such two-loop diagrams in LO QNS can lead to an inconsistency

[2] Our result in this case is exactly the same as that obtained recently by Andersen et al [27].

[3] This is equivalent to the quenched approximation.

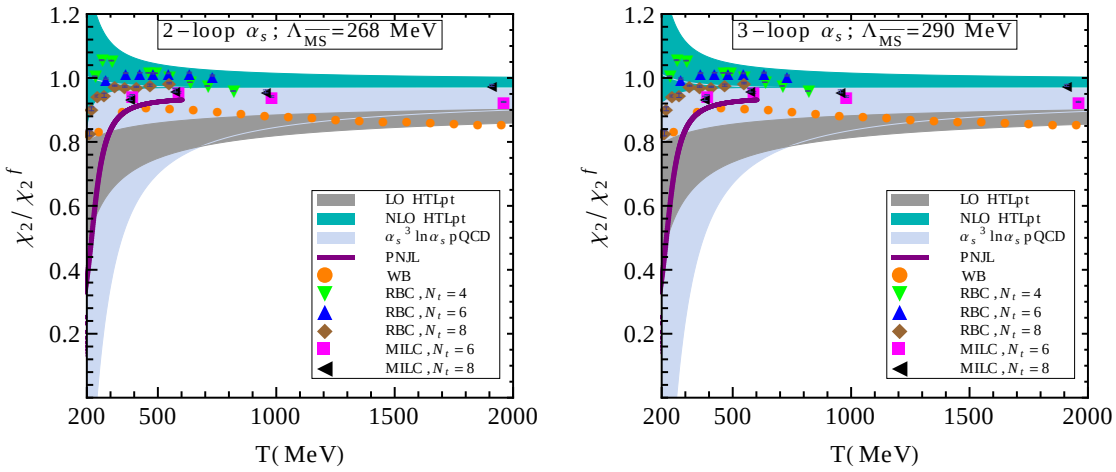

Figure 2. Same as Fig. 1 except the LO HTLpt QNS is replaced by the prescription specified in Eq. (4.6), which avoids the problem of over-counting in the LO HTLpt QNS (see text).

in the LO mass prescription in one-loop HTLpt and thus overcounts LO QNS. In what follows, as an alternative prescription, in the thermodynamic quantities which are related through exact thermodynamic relations either by derivatives or integrations with respect to μ or T of a given thermodynamic quantity, one identifies the mass parameters only after differentiations or integrations to preserve a given mass prescriptions in HTLpt.

Following the above prescription we can obtain LO QNS by performing derivatives on explicit μ dependence of one-loop pressure in (3.1) as

$$\chi_2^{\rm LO}(T) = \frac{d_F T^2}{3}\left[1 - \frac{3c_F}{8}\left(\frac{g}{\pi}\right)^2\right] = \chi_2^f\left[1 - \frac{1}{2}\left(\frac{g}{\pi}\right)^2\right] . \tag{4.6}$$

where $\chi_2^f = d_F T^2/3 = N_f T^2$. The above expression avoids over-counting in the LO HTLpt QNS. We plot the results of this prescription in Fig. 2. Since the over-counting resulted in an additional factor of 2 at LO (4.1), Fig. 2 displays only a small change to the LO HTLpt QNS compared to Fig. 1, particularly at smaller T.

The over-counting encountered at LO can be eliminated by pushing the calculation to NLO since the derivatives of the NLO mass parameters with respect to μ vanish (cf, Eq.(4.3)) due to the well-defined variational mass gap equations in (3.6) and (3.7). Moreover, the NLO result also reproduces the correct $\mathcal{O}(g^3)$ coefficient which can be seen from (4.3) using LO order masses as

$$\chi_2^{\rm NLO}(T) = \chi_2^f\left[1 - \frac{1}{2}\left(\frac{g}{\pi}\right)^2 + \sqrt{1+\frac{N_f}{6}}\left(\frac{g}{\pi}\right)^3 + \mathcal{O}(g^4) + \cdots\right] . \tag{4.7}$$

Nevertheless, we see in Fig. 1 and also in Fig. 2 that NLO HTLpt in (4.3) exhibits a modest improvement over the pQCD calculation shown, which is accurate to $\mathcal{O}(\alpha_s^3 \ln \alpha_s)$. However, the NLO χ_2 is higher than the LO one at higher temperature and it goes beyond the free gas value at lower temperatures. It should be mentioned that although the 2-loop

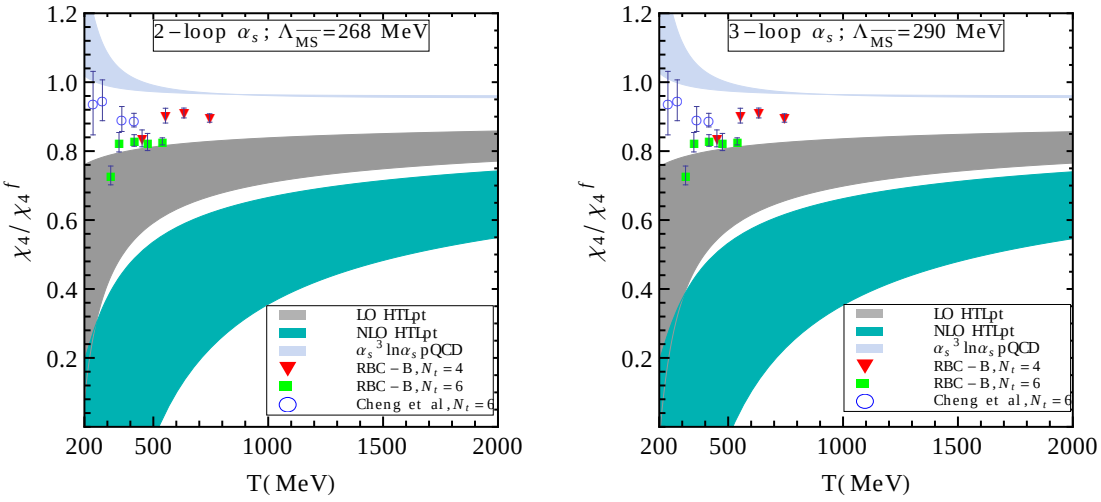

Figure 3. Left panel: χ_4 scaled by the free field value for LO and NLO HTLpt as given, respectively, in (4.2) and (4.4), 4-loop pQCD [8], and LQCD [11, 16] are plotted as a function of the temperature. The bands in HTLpt and pQCD are obtained by varying the $\overline{\rm MS}$ renormalisation scale (Λ) around its central value by a factor of two. We used $\Lambda_{\overline{\rm MS}} = 268$ MeV and 2-loop α_s for HTLpt and pQCD. Lattice QCD results [11, 16] are represented by symbols. Right panel: Same as left panel but using 3-loop α_s and $\Lambda_{\overline{\rm MS}} = 290$ MeV.

calculation rectifies the LO over-counting, it does so by pushing the problem to higher order in g. The reason can be understood in the following way: in HTLpt the loop and coupling expansion are not symmetrical, therefore at a given loop order there are contributions from higher orders in coupling. Since the NLO HTL pressure and thus QNS is only strictly accurate to order $\mathcal{O}(g^3)$ there is over-counting occurring at higher orders in g, namely at $\mathcal{O}(g^4)$ and $\mathcal{O}(g^5)$. A next-to-next-to-leading order (NNLO) HTLpt calculation would fix the problem through $\mathcal{O}(g^5)$ thereby guaranteeing that, when expanded in a strict power series in g, the HTLpt result would reproduce the perturbative result order-by-order through $\mathcal{O}(g^5)$.

In Fig. 3 we plot the fourth-order QNS (χ_4) scaled by the corresponding free gas value for HTLpt as given in (4.2) and (4.4), pQCD, and LQCD. Both the HTLpt and pQCD results exhibit a very weak dependence on the choice of order of the running of α_s and thus $\Lambda_{\overline{\rm MS}}$. Nevertheless, the HTLpt results are found to be far below the pQCD result [8] which is accurate to $\mathcal{O}(\alpha_s^3 \ln(\alpha_s))$ and the LQCD results [11, 16]. Obviously, the LO χ_4 in (4.2) suffers from severe over-counting due to the inclusion of μ derivatives of the LO mass parameters that spoil the mass prescription in LO HTLpt. Also, the correction to χ_4 when going from LO to NLO is quite large. This is again due to the survival of the double derivatives of the mass parameters with respect to μ in (4.4), which again violate the NLO mass prescription obtained through the variational mass gap equations in (3.6) and (3.7). As discussed earlier if one suppresses these derivatives of mass parameters, one would rectify the over-counting in the contributions to χ_4 in LO HTLpt. With this recipe, i.e., performing the explicit μ derivatives of the one-loop pressure in (3.1), the LO χ_4 can

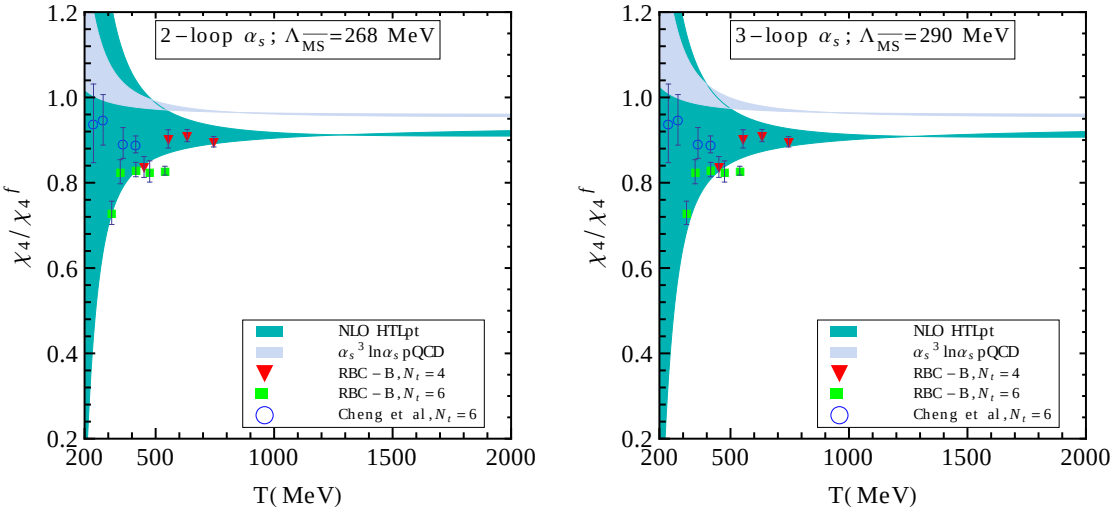

Figure 4. Left panel: χ_4 scaled by the free field value for NLO HTLpt in Eq.(4.9), 4-loop pQCD [8], and LQCD [11, 16] are plotted as a function of the temperature. The bands in HTLpt and pQCD are obtained by varying the $\overline{\rm MS}$ renormalisation scale (Λ) around its central value by a factor of two. We used $\Lambda_{\overline{\rm MS}} = 268$ MeV and 2-loop α_s for HTLpt and pQCD. Lattice QCD results [11, 16] are represented by symbols. Right panel: Same as left panel but using 3-loop α_s and $\Lambda_{\overline{\rm MS}} = 290$ MeV.

be obtained

$$\chi_4^{\rm LO}(T) = \chi_4^f[1 - \mathcal{O}(g^6)]\,, \tag{4.8}$$

where the HTL correction appears only in $\mathcal{O}(g^6)$ since there is no explicit μ^4 dependence in the terms up to $\mathcal{O}(g^4)$ in one-loop HTL pressure in (3.1) (such contributions only appear starting at $\mathcal{O}(g^6)$).

On the other hand the NLO χ_4 can be obtained through the explicit μ derivatives of the NLO pressure in (3.4) as

$$\begin{aligned}\chi_4^{\rm NLO}(T) = \frac{d_A}{4\pi^2}\Bigg[8\frac{d_F}{d_A} + \frac{\alpha_s}{\pi}s_F\Bigg\{ &-12 + 80\hat{m}_D^2(0)\left(\ln\frac{\hat{\Lambda}}{2} - 1.0811\right)(\zeta(5) - \zeta(3)) \\ &+6\left(19.836 + 288\ln\frac{\hat{\Lambda}}{2}\right)\hat{m}_q^2(0) \\ &-4\hat{m}_D^3(0)\left[31\zeta(5) - 120\left(\frac{\zeta'(-1)}{\zeta(-1)} + \ln\hat{m}_D(0)\right)(\zeta(5) - \zeta(3))\right]\Bigg\}\Bigg]\,,\end{aligned} \tag{4.9}$$

where, as expected, the correct order g^2 term appears along with higher orders, viz., $\mathcal{O}(g^4)$ and $\mathcal{O}(g^5)$; however, no $\mathcal{O}(g^3)$ term appears.

In Fig. 4 we show the result of this modified prescription for the NLO χ_4 (4.9). As can be seen from this figure when one avoids the over-counting there is a remarkable improvement compared to Fig. 3 and the result exhibits a better agreement with LQCD

data [11, 16]. Since it is only accurate up to $\mathcal{O}(g^2)$, higher orders still suffer from over-counting. This suggests that one may need to go beyond NLO to NNLO HTLpt in order to fix $\mathcal{O}(g^3)$, full convergence, and perhaps even better agreement with pQCD. A similar situation was seen with the pressure at zero chemical potential for which the NNLO HTLpt result provided a dramatic improvement over the NLO result [36]; however, there is no guarantee that a similar dramatic improvement will occur for QNS. The only way to know is to extend the calculation for the finite temperature and chemical potential HTLpt thermodynamic functions to NNLO. Work along these lines is currently underway.

5 Conclusion and Outlook

In this paper we have obtained the second- and fourth-order QNS from the NLO HTLpt pressure obtained in a high temperature expansion through $\mathcal{O}[(\mu/T)^4]$. Analytic expressions were found for both $\chi_2^{\rm LO}$ and $\chi_4^{\rm LO}$ within LO HTLpt. Our result for $\chi_2^{\rm LO}$ (4.1) is in agreement with the results obtained previously by Andersen et al. [27]; however, we have found that the perturbative mass prescription used therein slightly over counts the LO QNS, since μ derivatives of the mass parameters appear which should not if a proper variational mass prescription is employed. For the same reason the $\chi_4^{\rm LO}$ in (4.2) suffers from over-counting through all orders to $\mathcal{O}(g^4)$. In this work we proposed a prescription which rectifies this over-counting at LO by requiring the necessary derivatives of the mass to vanish. The LO result for χ_2 shows reasonable agreement with available LQCD data [9, 11, 15]; however, at this point in time there is still a fairly sizable variation of this quantity between the different lattice groups. Moving forward it would seem that a detailed analysis of the uncertainties in the various LQCD calculations is necessary before detailed conclusions can be drawn.

At NLO we obtained semi-analytic expressions for $\chi_2^{\rm NLO}$ and $\chi_4^{\rm NLO}$ and, after numerically solving the necessary variational gap equations for the mass parameters m_D and m_q, we obtained our results for $\chi_2^{\rm NLO}$ in (4.3) and $\chi_4^{\rm NLO}$ in (4.4). Unlike the LO results, our NLO calculation takes into account dynamical quark contributions by including two-loop graphs which involve fermion loops; however, they suffer from the same problem that NLO HTLpt calculations at zero chemical potential faced: the NLO χ_2 in (4.3) gets $\mathcal{O}(g^3)$ correct but the $\mathcal{O}(g^4)$ and $\mathcal{O}(g^5)$ contributions are incorrect if they are expanded out in a strict power series in g. As a result, our NLO result for χ_2 scaled to the free limit is closer to unity than the corresponding LO result and only shows a weak dependence on the chosen value of the renormalization scale. Our NLO result for χ_4 (cf, eq.(4.4)) in which μ derivatives of the variational mass parameters survive is significantly below the pQCD and lattice data. As we discussed, this occurs because of severe over-counting since higher order corrections contribute through the derivatives of the mass parameters with respect to μ. Once the NLO mass prescription is enforced using the method proposed herein, the NLO χ_4 (4.9) becomes accurate to $\mathcal{O}(g^2)$, which was missing in LO HTLpt (4.8). Nevertheless, no $\mathcal{O}(g^3)$ term shows up at NLO in χ_4 (4.9), whereas higher orders, viz., $\mathcal{O}(g^4)$ and $\mathcal{O}(g^5)$ suffer from over-counting like NLO χ_2.

As was the case with the pressure at zero chemical potential, fixing this problem will require going to NNLO. In the case of the zero chemical potential pressure, performing such a calculation resulted in much improved agreement between HTLpt and LQCD calculations above $\sim 2\,T_c$. At the very least a NNLO calculation will fix the over-counting problems through $\mathcal{O}(g^5)$. Whether going to NNLO will improve the agreement of the HTLpt χ_2 and χ_4 predictions with LQCD results will have to remain an open question for the time being. Work on the NNLO calculation has begun, but being a NNLO calculation, care and patience must be applied in equal measure.

Acknowledgments

We thank Anirban Lahiri for providing the QNS data from the PNJL model, Peter Petreczky for providing the LQCD data for the fourth-order QNS, and Nan Su for useful discussions during the course of this work. M.S. was supported by NSF grant No. PHY-1068765.

References

[1] M. Asakawa, U. Heinz, and B. Müller, Phys. Rev. Lett. **85**, 2072 (2000); S. Jeon and V. Koch, Phys. Rev. Lett. **85**, 2076 (2000); M. Cheng, P. Hendge, C. Jung, F. Karsch, O. Kaczmarek, E. Laermann, R. D. Mawhinney and C. Miao *et al.*, Phys. Rev. D **79**, 074505 (2009).

[2] D. Forster, *Hydrodynamics, Fluctuation, Broken Symmetry and Correlation Function* (Benjamin/Cummings, Menlo Park, CA, 1975); H. B. Callen and T. A. Welton, Phys. Rev. **122**, 34 (1961); R. Kubo, J. Phys. Soc. Jpn. **12**, 570 (1957).

[3] L. McLerran, Phys. Rev. D **36**, 3291 (1987).

[4] T. Hatsuda and T. Kunihiro, Phys. Rep. **247**, 221 (1994); T. Kunihiro, Phys. Lett. B **271**, 395 (1991).

[5] M. A. Stephanov, K. Rajagopal, and E. Shuryak, Phys. Rev. Lett. 81, 4816 (1998); Phys. Rev. D. 60, 114028 (1999); M. A. Stephanov, Phys. Rev. Lett. 102, 032301 (2009).

[6] T. Toimela, Int. J. Theor. Phys. **24**, 901 (1985).

[7] J. I. Kapusta and C. Gale, *Finite Temperature Field Theory Principle and Applications* (Cambridge University Press, Cambridge, 1996), 2nd ed.

[8] A. Vourinen, Phys. Rev. D**67**, 074032 (2003).

[9] Sz. Borsányi, G. Endrődi, Z. Fodor, S.D. Katz, S. Krieg, C. Ratti and K.K. Szabó, JHEP **1208**, 053 (2012).

[10] A. Bazavov, H.T. Ding, P. Petreczky, J.Phys.Conf.Ser. **389** (2012) 012017; P. Petreczky, J.Phys. G **39** (2012) 093002

[11] P. Petreczky, P. Hegde, and A. Velytsky, Proc. Sci., **LAT2009** (2009) 159 [arXiv:0911.0196].

[12] A. Bazavov et al., Phys.Rev. D **86** (2012) 034509.

[13] C. R. Allton et al., Phys. Rev. D **71**, 054508 (2005).

[14] A. Bazavov et al., Phys. Rev. D **80**, 014504 (2009).

[15] C. Bernard et al. (MILC Collaboration), Phys. Rev. D **71**, 034504 (2005).

[16] M. Cheng et al., Phys. Rev. D**79**, 074505 (2009).

[17] R. Gavai and S. Gupta, Phys. Rev. D **64**, 074506 (2001); **65**, 094515 (2002); R. Gavai, S. Gupta, and P. Majumdar, *ibid.* **65**, 054506 (2002).

[18] K. Kusaka, Phys. Lett. B**269**, 17 (1991).

[19] H. Fujii, Phys. Rev. D **67**, 014028 (2003); C. Sasaki, B. Friman, and K. Redlich, *ibid.* **75**, 054026 (2007); C. Ratti et al., Phys. Lett. B **649**, 57 (2007).

[20] S. Mukherjee, M. G. Mustafa, R. Ray, Phys. Rev. D **75** (2007) 094015, S.K. Ghosh, T. K. Mukherjee, M. G. Mustafa, R. Ray, Phys. Rev. D**73** (2006) 114007; Phys. Rev. D **77** (2008) 094024.

[21] S. Chatterjee, K. A. Mohan, Phys.Rev. D **85** (2012) 074018; ⟨arXiv:1201.3352⟩.

[22] A. Bhattacharyya, P. Deb, A. Lahiri, R. Ray, Phys.Rev. D **82** (2010) 114028; Phys.Rev. D **83** (2011) 014011.

[23] P. Chakraborty, M. G. Mustafa, and M. H. Thoma, Eur. Phys. J. C. **23**, 591 (2002); Phys. Rev. D **68**, 085012 (2003).

[24] N. Haque, M. G. Mustafa and M. H. Thoma, Phys. Rev. D**84**, 054009 (2011); N. Haque and M. G. Mustafa, Nucl. Phys. A**862-863**, 271 (2011); N. Haque and M. G. Mustafa, ⟨arXiv:1007.2076 [hep-ph]⟩.

[25] J.-P. Blaizot, E. Iancu, and A. Rebhan, Phys. Lett. B **523** (2001) 143; Eur. Phys. J. C **27** (2003) 433.

[26] Y. Jiang, H.-x. Zhu, W.-m Sun, and H.-s. Zong, J. Phys. G **37**, 055001 (2010).

[27] J. O. Andersen, S. Mogliacci, N. Su and A. Vuorinen, ⟨arXiv:1210.0912 [hep-ph]⟩.

[28] M. He, D. K. He, H. T. Feng, W. M. Sun, and H. S. Zong, Phys. Rev. D **76** (2007) 076005; M. He, J. F. Li, W. M. Sun, and H. S. Zong, Phys. Rev. D **79** (2009) 036001; D. K. He, X. X. Ruan, Y. Jiang, W. M. Sun, and H. S. Zong, Phys. Lett. B **680** (2009) 432; Y. Jiang, L.-J. Luo, H.-S. Zong, JHEP **1102** (2011) 066.

[29] Kyung-il Kim, Y. Kim, S. Takeuchi, T. Tsukioka, Prog. Theor. Phys. **126** (2011) 735-751; L.-X. Cui, S. Takeuchi, Y.-L. Wu, Phys. Rev. D **84** (2011) 076004; Y. Kim, S. Takeuchi, T. Tsukioka Prog. Theor. Phys. Suppl. **186** (2010) 498-503.

[30] B.-J. Schäfer and J. Wambach, Phys. Rev. D**75**, 085015 (2007); B.-J. Schäfer, M. Wagne, and J. Wambach, Phys. Rev. D**81**, 074013 (2010).

[31] M. Bluhm, B. Kampfer and G. Soff, Phys. Lett. B **620**, 131 (2005); M. Bluhm and B. Kampfer, Phys. Rev. D **77**, 114016 (2008).

[32] E. Braaten and R. D. Pisarski, Nucl. Phys. **B337**, 569 (1990); Phys. Rev. Lett. **64**, 1338 (1990).

[33] E. Braaten and R. D. Pisarski, Phys. Rev. D **45**, R1827 (1992).

[34] J. O. Andersen, E. Braaten, and M. Strickland, Phys. Rev. Lett. **83**, 2139 (1999); Phys. Rev. D **61**, 014017 (1999); Phys. Rev. D **61**, 074016 (2000).

[35] J. O. Andersen, E. Petitgirard, and M. Strickland, Phys. Rev. D**66** (2002) 085016; Phys. Rev. D**70**, 045001 (2004).

[36] N. Su., J. O. Andersen, and M. Strickland, Phys. Rev. Lett. **104**, 122003 (2010); J. O. Andersen, M. Strickland, and N. Su, JHEP **1008**, 113 (2010); J.O. Andersen, L.E. Leganger, M. Strickland and N. Su, Phys. Lett. B **696**, 468 (2011); J. O. Andersen, L. E. Leganger, M. Strickland and N. Su, JHEP **1108**, 053 (2011); J. O. Andersen, L. E. Leganger, M. Strickland and N. Su, Phys. Rev. D **84**, 087703 (2011).

[37] N. Haque, M. G. Mustafa and M. Strickland, ⟨arXiv:1212.1797[hep-ph]⟩.

[38] P. Chakraborty, M. G. Mustafa, and M. H. Thoma, Phys. Rev. D **67**, 114004 (2003).

[39] A. Bazavov *et al.*, Phys. Rev. D **86**, 114031 (2012).